LASER INDUCED DIFFUSIBLE RESISTANCE: DEVICE CHARACTERIZATION AND PROCESS MODELING

M. Meunier*[a,b], M. Cadotte [a], M. Ducharme [a], Y. Gagnon [b], and A. Lacourse [b]
[a]École Polytechnique de Montréal, Département de Génie Physique, Case Postale 6079, Succursale. Centre-ville, Montréal (Québec), Canada, H3C 3A7
[b]LTRIM-Technologies, 440 Blvd Armand Frappier, suite 140, Laval, Québec, Canada, H7V 4B4

ABSTRACT

Highly accurate resistances can be made by iteratively laser inducing diffusion of dopants from the drain and source of a gateless field effect transistor into the channel, thereby forming an electrical link between two adjacent p-n junction diodes. We show that the current-voltage characteristics of these new microdevices are linear at low voltages and sublinear at higher voltages where carrier mobility is affected by the presence of high fields. A process model is proposed involving the calculation of the laser melted region in which the dopant diffusion occurs. Experimental results are well described by the proposed model.

Keywords: Laser trimming, microelectronics, resistance

INTRODUCTION

Due to the inevitable fabrication process variabilities, microelectronics circuit functionality are very often altered, resulting in chips off specifications or useless. Because of the intrinsic characteristics of digital microelectronics, which essentially consists of low (or 0) and high (or 1) voltages, they can be built more robust to these fabrication variabilities than analog circuits for which high accurate components are required. To keep pace with the rapid growth of digital microelectronics, trimming techniques have to be used to accurately adjust some microdevices' characteristics for analog microelectronics. We have recently proposed a new laser technique to finely tune analog microelectronics circuits which presents the advantages of being very accurate, using very small die area, and being easily integrated into any actual CMOS process without additional steps [1,2]. A patent disclosing the detailed device structure and creation method has been recently accepted [3].

In this paper, after reviewing the principle of the technique, we present the electronic characterization and the modeling of these new microdevices and show that they present excellent current-voltage linear behavior at usual microelectronics voltages. Furthermore, process modeling based on the laser induced silicon melted region calculation is detailed and successfully compared to experimental results.

PRINCIPLE OF THE LASER TRIMMING METHOD

The laser trimming technique, which has been described previously [1,2] is performed on a device structure consisting of a MOSFET, without the gate, fabricated by a conventional CMOS process. For an n-type resistor, the device structure consist of two highly doped regions, separated by 2L and formed by implantation into a p-well, resulting into two p-n junctions facing each other. Before performing laser trimming, the only current that can flow through the device is the p-n junctions leakage current, resulting essentially in an open circuit. Focusing a laser beam on the gap region between the two junctions causes melting of the silicon, resulting in dopant diffusion from the highly doped regions to the lightly-doped gap region. Upon removal of the laser light, the silicon solidifies and freezes in place, leaving the diffused dopants in a new special distribution forming an electrical link between the highly doped regions. This laser-diffused link constitutes the trimmed resistor. Tight control of process parameters is necessary to create efficiently these laser diffusible links while avoiding damage to adjacent devices and structures. These parameters are the laser spot size, the pulse duration, the laser power, the number of laser expositions and the position of the laser spot relative to the device. By varying the parameters between each laser intervention, one can accurately control the tuning of the device. The laser system consisting of the laser, the necessary optics to focus the beam on the microelectronics chip and a X-Y-Z computer controlled positioner has been described previously [1,2].

*meunier@phys.polymtl.ca, phone: 514-340-4711 ext 4971

Photon Processing in Microelectronics and Photonics, Koji Sugioka, Malcolm C. Gower, Richard F. Haglund, Jr., Alberto Piqué, Frank Träger, Jan J. Dubowski, Willem Hoving, Editors, Proceedings of SPIE Vol. 4637 (2002) © 2002 SPIE · 0277-786X/02/$15.00

DEVICE CHARACTERIZATION

Figure 1 shows some typical microdevices that have been tuned with the laser. These circuits, which have no specific electronic functionality other than testing the devices, consist essentially of arrays of gateless MOSFET's with a source to drain distance of 1.7μm. Figure 1 (a) has been taken by an optical microscope and shows that the top interdielectrics layers are almost not affected by the laser. Figure 1 (b) shows an image taken by a Focus Ion Beam (FEI Company). The two black spots represent holes which have been deliberately made with the laser to cut electrical links. Again, the laser process for making a diffusible resistance has essentially no effect on the interdielectrics. Figure 2 shows images produced with an Atomic Force Microscope (AFM) and a Scanning Capacitance Microscope (SCM) (Digital Instruments, Dimension 3100 model) of a laser diffused resistance, where all outer dielectric layers have been removed by an HF etch. Five laser pulses with a beam waste of 0.9μm were used in this experiment and the laser parameters were maintained at a duration of 1μs and a laser power of 0.75W incident on the surface of the chip (estimated at 0.65 W on the silicon surface). While the AFM image reveals no significant deformation of the p-well, the SCM image shows clearly that dopants, represented by a dark gray, have diffused from the two n+ regions into the p-channel. The diffused region is about $1.1 \pm 0.2\,\mu m$ in diameter.

Figure 1 (a)
Optical microscope image of a laser induced modification of the device. The interdielectrics are essentially unaffected.

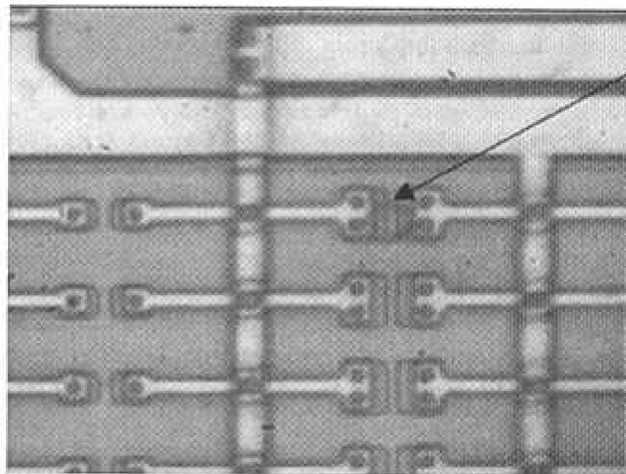

Figure 1 (b)
Focus ion beam image of a laser induced diffusible resistance. The two black spots on the left are due to two deliberate laser cuts. In the middle, three laser irradiations were performed on the microdevices. The interdielectrics layers are essentially unaffected.

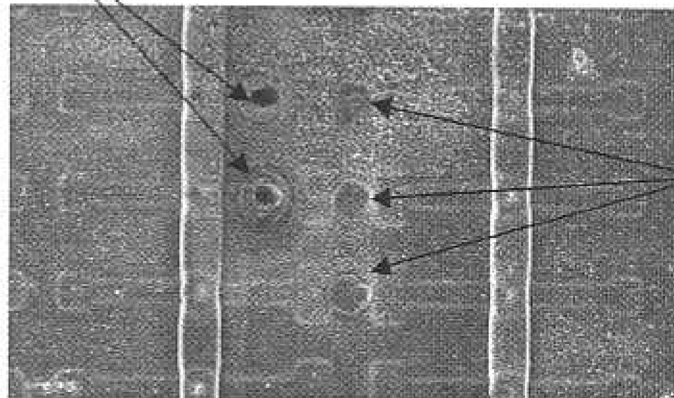

Figure 1 Images of laser induced diffusible resistances

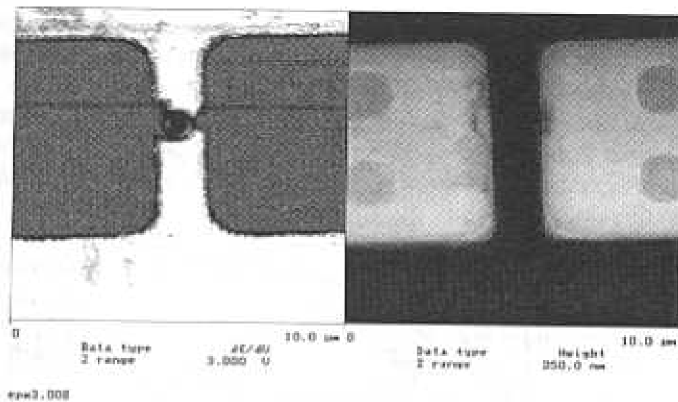

Figure 2 : SCM image (left) and corresponding AFM image (right) of a laser induced diffusible resistance. The n-channel is clearly visible on the SCM image whereas topography (AFM) reveals no significant deformation of the p-well. (The distance between the source and the drain is 1.7µm)

Current-voltage (I-V) characteristics have been measured using a Hewlett Packard 4155A semiconductor parameter analyzer. The current-voltage curves of typical laser diffusible resistances are presented in Figure 3. Lower resistance devices (lower than few kΩ) present an excellent linearity over the range of voltages normally used in microelectronics (±1.5V), while higher resistance devices show non-linear effects and a relatively small (-0.3V to 0.3V) linear region. In Figure 3(b), I-V characteristics are plotted up to relatively large applied voltages. They show a non-linear behavior primarily related to the carrier velocity saturation at moderate fields and to an avalanche effect at high fields, reducing the resistance which permits a greater current to flow into the device.

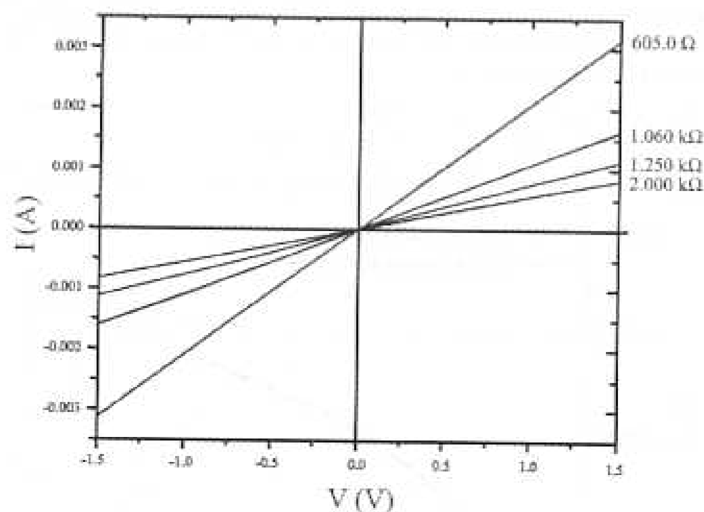

(a)

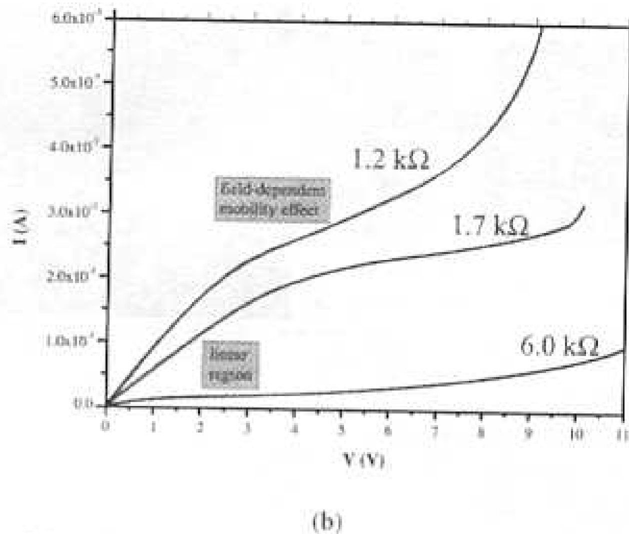

(b)

Figure 3: Current-voltage characteristics of three laser diffusible resistances at (a) low voltages (< 1.5V) and (b) at high voltages

In order to more deeply understand these I-V characteristics, these created devices can easily be associated to a n+-v-n+ diode where the laser diffused region acts as the n-doped region [4]. At low applied voltages, a 1D finite element analysis shows that a monotonous electric field is created throughout the v region generating a drift carrier current, resulting in a linear I-V curve. As the applied voltage increases, a more intense electric field, as large as 5kV/cm, is applied on the carriers, especially near the junctions where the presence of space charges adds to the magnitude of the field. The bending of the I-V is attributed to the saturation of the carriers velocity at these higher fields. To verify this, a 2D finite element quasi-stationary analysis has been carried out with the computer program ISE TCAD [5], using the doping level dependant mobility model of Masetti et al.[6] and the velocity saturation model of Canali et al [7]. As shown in figure 4, simulation calculations are in very good agreement with experimental results when a uniform dopant concentration of 1.5×10^{18} cm^{-3} is assumed. The theoretical analysis is being pursued on the I-V characteristics at even higher fields, especially after the current saturation, where space-charge-limited currents are expected to be important.

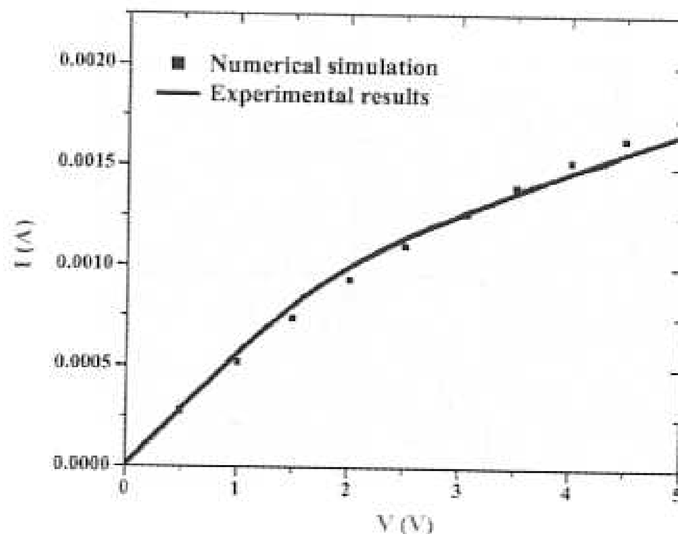

Figure 4: 2D simulation of the I-V characteristics of a laser diffusible resistance of 1.802 kΩ

PROCESS CHARACTERIZATION AND MODELING

Modeling this process involves a time-dependent three-dimensional (3D) calculation of the temperature due to the laser irradiation [8], followed by a dopant distribution calculation using Fick's law. A simple model must include the effects of the laser power, beam waist and exposure time as well as the geometric characteristics of the initial structure. Device characteristics can then be evaluated by solving the three differential coupled equations to obtain the 3D distributions of electron and hole concentrations, as well as the electric field in the device presenting a non-uniform dopant distribution. In addition, modeling must also include the possibility of varying the laser beam location and power from pulse to pulse to obtain the desired device characteristics.

Some insight on process modeling can be obtained by using careful approximations. We consider the effect of a focused laser beam incident on a n+-p-n+ silicon structure, resulting in the diffusion of dopants into silicon. Because the diffusion coefficient of dopants in liquid Si is almost seven orders of magnitude higher than that of crystalline Si, we assume that only dopants in the silicon melt diffuse [9]. During the laser pulse, the silicon melt dimension increases and then decreases as the pulse ends. Therefore, we propose that only the maximum melted region (as denoted by r_{melt} on the Si surface) has to be determined in the temperature calculation; the dopants located outside this region are assumed to be immobile. As the pulse duration t gets longer, dopants with a diffusion coefficient D_d will have more time to diffuse over a length of

$$r_D = 2\sqrt{D_d t} \qquad (1)$$

in the entire melted region, yielding a more uniform dopant distribution. For instance, Arsenic, the major dopant in the n+ regions of the investigated structures, presents diffusion constants between D_d=3.3x10^{-4}cm^2/s and 6.8x10^{-3}cm^2/s corresponding respectively to the fusion temperature (T=1683K) and to a reasonable temperature of molten Si (T=3000K) [9]. Equation (1) gives in these conditions:

$$r_D(\mu m) = 0.36\sqrt{t(\mu s)} \quad \text{for } T=1683 \text{ K} \qquad (2)$$

and

$$r_D(\mu m) = 1.65\sqrt{t(\mu s)} \quad \text{for } T=3000 \text{ K} \qquad (3)$$

suggesting that laser pulses of the order of a microsecond are required for uniform dopant distribution over a fraction of a micrometer.

To calculate the maximum melted region one has to solve the basic energy balance equation including the laser source term as well as the conduction, convection and radiation heat losses. Since the radiation term is essentially negligible compared to the conduction term and since, in a first approximation, we can neglect convection because the pulse melting time is lower than few µs, the energy balance equation can be written as [8]:

$$\rho c\frac{\partial T}{\partial t} = \nabla \bullet [\kappa \nabla T] + S(x,y,z,t) \qquad (4)$$

where ρ, c, κ denote density, specific heat and thermal conductivity, respectively. The heat source S is given by:

$$S(x,y,z,t) = [1-R]\,Q(x,y)\,f(z)\,g(t) \qquad (5)$$

$$Q(x,y) = \frac{P}{\pi w^2}\exp\left[-\frac{x^2+y^2}{w^2}\right] \qquad (6)$$

$$f(z) = \alpha e^{-\alpha z} \qquad (7)$$

where R is the surface reflectivity, P the incident power, w the 1/e laser spot radius, α the optical absorption coefficient and $g(t)$ the temporal laser profile (in this case we assume a rectangular pulse). Temperature dependent thermal conductivity can be eliminated from equation (4) using a Kirchhoff transform [10]:

$$\Theta(T) = \int_{T_0}^{T} \frac{\kappa(T')}{\kappa(T_0)} dT'$$

(8)

where $\Theta(T)$ is called the linear temperature and T_0 is the initial temperature. The heat equation is then solved using Green's function method [11]. The solution has been calculated by Cohen et al [12] and is given by:

$$\Theta(x,y,z,t) = \frac{(1-R)P\alpha}{2\pi^{3/2}\kappa(T_0)} \int_0^{\sqrt{4Dt}} d\xi\, I(z,\xi) \frac{\exp[-(x^2+y^2)/(\xi^2+w^2)]}{\xi^2+w^2}$$

$$I(z,\xi) = \frac{\sqrt{\pi}}{2}\xi \exp(\alpha^2\xi^2/4)\left[e^{-\alpha z}\left(1-erfc\left(\frac{\alpha\xi}{2}-\frac{z}{\xi}\right)\right)+e^{\alpha z}\left(1-erfc\left(\frac{\alpha\xi}{2}+\frac{z}{\xi}\right)\right)\right]$$

(9)

where *erfc( )* is the complementary error function, *D* is the thermal diffusivity and

$$\xi = \sqrt{4D(t-t')}$$

(10).

As it is, equation (9) does not take into account the temperature dependence of Si properties or latent heat of fusion. However, by using an adiabatic approximation [13], it is possible to partially consider these in the calculation. The temporal integral of equation (8) is subdivided into small time segments, each lasting Δt_i. These segments cumulatively add up to give the total temperature at the designated time. Each segment depends on the total temperature reached by the preceding segment. In this way, silicon properties can be adjusted to the temperature reached after each segment. The time intervals Δt_i are chosen so as to limit the temperature only to rise a few Kelvins. The main draw back to this method is that the properties of Si depend on temperature which in turn depends on time and position. The adiabatic approximation takes care of the temperature variation with time, but not with position. As for latent heat of fusion (L), it is taken into account with the use of an energetic criterion [14]. If the fusion temperature (T_f) of silicon is reached, subsequent temperature increases are converted into enthalpy:

$$H = \int_{T_f}^{T} (\rho c)_{T_f}\, dT'$$

(11)

where ρc is evaluated at T_f. As long as the energy accumulated is less than the latent heat of fusion, the material is considered still in the melt transition. When $H \geq L$, the liquid phase is reached and subsequent temperature rise calculations return to normal (albeit with liquid silicon properties).

While our calculation approach using equation (9) is basically not rigorous, it is expected to be more accurate than using equation (9) without temperature dependent properties, as it will be shown when calculations are compared to experimental results. As an example, for the conditions given in figure 2, the model using constant silicon properties predicted that the silicon would not melt, which is obviously not the case. However, our approach gives a calculated radius of 0.5μm, which is very close to the observed dopant diffused area of 0.55 ± 0.1μm seen in Figure 2.

Another way to compare experimental and theoretical calculations is to determine the conditions which give a fixed melted radius. This can be done in the following manner. Before laser irradiation, the resistance of the microdevice has essentially an infinite value. According to the proposed model, process parameters must be such that the melted region must reach the source and the drain before the dopants begin to diffuse into the channel. For a determined laser power, a minimum pulse width is required to diffuse sufficient dopants to produce a resistance. We have performed measurements on microdevices with a 1.7 μm source to drain distance and for source and drain initial concentrations of 5×10^{19} cm^{-3}. Figure 6 shows experimental results to produce a resistance of a finite value (readable on the multimeter, i.e. between 10^7 and 10^8 Ω) with only <u>one</u> laser irradiation. Note that to obtain 10^8 Ω on the multimeter, a silicon resistivity of 10^3 Ωcm is needed corresponding to a dopant concentration as low as 10^{13} cm^{-3} in the channel on the average [15]. Even at the shortest pulse width of 0.07 μs (at few Watts on figure 6), we estimate using equation (3) that this time is long enough to assure sufficient dopant diffusion to be observed at the multimeter. The dashed line on figure 5 corresponds to the calculated time and power for a melted radius of 0.85μm (half the distance source to drain) using equation (9). The full line corresponds to our calculation taking into consideration all silicon properties dependence with temperature. The agreement between the results and our calculation (full line) is very good and furthermore supports the proposed model that the diffusion into the melted region is the main mechanism controlling the process.

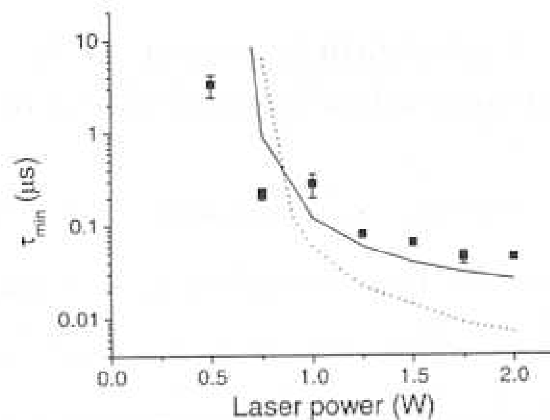

Fig. 5: Minimum time needed to create a resistance of finite value (i.e. between 10^7 and 10^8 Ω) as a function of laser power for one laser irradiation. Small squares are experimental results and lines are calculated from the model with (full line) and without (dotted line) latent heat of fusion and thermally dependent Si properties.

CONCLUSIONS

Highly accurate resistances compatible with CMOS technology can be easily made by laser inducing dopant diffusion. These new microdevices have very linear I-V curves at the usual microelectronics operating voltages and present non-linear behavior due to carrier velocity saturation followed by avalanche effects. We clearly showed that the process is based on the dopant diffusion into the melted silicon and our calculations are in good agreements with experimental results.

ACKNOWLEDGMENTS

The authors are grateful to J.P. Lévesque and Hugo St-Pierre for technical assistance and Yvon Savaria for stimulating discussions. The authors whish to thank Digital Instruments and FEI Company for AFM-SCM and FIB measurements respectively.

REFERENCES

[1] M. Meunier, Y. Gagnon, Y. Savaria, A. Lacourse and M. Cadotte, Proc. of SPIE, **4274**, 384 (2001)
[2] M. Meunier, Y. Gagnon, Y. Savaria, A. Lacourse and M. Cadotte, accepted in Applied. Surface Science, (2001)
[3] Y. Gagnon, M. Meunier, Y. Savaria, , "Method and Apparatus for Iteratively Selectively Tuning the Impedance of Integrated Semiconductor Devices Using a Focused Heating Source", US Patents **6,329,272** and PCT # 06042-002-WO-1 by LTRIM Technologies Inc. (2001)
[4] A. Van Der Ziel, "Space-Charge-Limited Solid-State Diode", Semiconductors and Semimetals, Ch.3 (1980)
[5] ISE TCAD 7.0, ISE Integrated Systems Engineering, AG, Switzerland, www.ise.com
[6] G. Masetti, M. Severi, and S. Solmi, "Modeling of Carrier Mobility Against Carrier Concentration in Arsenic-, Phosphorus- and Boron-Doped Silicon", IEEE Trans.Electron Devices, **ED-30**, 764-769 (1983)
[7] C. Canali, G. Majni, R. Minder, and G. Ottaviani, "Electron and hole drift velocity measurements in silicon and their empirical relation to electric field and temperature", IEEE Trans. ED, pp. 1045-1047 (1975)
[8] D. Bäuerle, Laser Processing and Chemistry, 3rd ed., Springer, Berlin (2000)
[9] H. Kodera, Jap. J. Appl. Phys., **2**, 212 (1963)
[10] H.S. Carslaw and J.C. Jaeger, "Conduction of Heat in Solids", Clarendon Press, Oxford (1988).
[11] E. Butkov, "Mathematical Physics", Addison-Wesley, Reading (1968)
[12] S.S. Cohen, P.W. Wyatt, G.H. Chapman and J.M. Canter, IEEE Trans. Electron Devices **35**, 1533 (1988)
[13] D.M. Kim, R.R. Shah and D.L. Crosthwait, J. Appl. Phys **51**, 3121 (1980)
[14] J.E. Moody and R.H. Hendel, J. Appl. Phys. **53**, 4364 (1982)
[15] see for example, Robert F. Pierret, "Advanced Semiconductor Fundamentals", Modular Series on Solid State Devices, volume VI (1989)